

# Coexpression of heparanase activity, cathepsin L, tissue factor, tissue factor pathway inhibitor, and MMP-9 in proliferative diabetic retinopathy

Ahmed M. Abu El-Asrar,<sup>1,2</sup> Mohammad Mairaj Siddiquei,<sup>1</sup> Mohd Imtiaz Nawaz,<sup>1</sup> Gert De Hertogh,<sup>3</sup> Ghulam Mohammad,<sup>1</sup> Kaiser Alam,<sup>1</sup> Ahmed Mousa,<sup>1</sup> Ghislain Opdenakker<sup>4</sup>

<sup>1</sup>Department of Ophthalmology, College of Medicine, King Saud University, Riyadh, Saudi Arabia; <sup>2</sup>Dr. Nasser Al-Rashid Research Chair in Ophthalmology; <sup>3</sup>Laboratory of Histochemistry and Cytochemistry, University of Leuven, KU Leuven, Leuven, Belgium; <sup>4</sup>Rega Institute for Medical Research, Department of Microbiology and Immunology, University of Leuven, KU Leuven, Leuven, Belgium

**Purpose:** Heparanase cleaves heparan sulfate side chains of heparan sulfate proteoglycans, activity that is implicated in angiogenesis. Proteolytic cleavage of proheparanase by cathepsin L leads to the formation of catalytically active heparanase. We investigated the expression levels of heparanase enzymatic activity and correlated these with the levels of cathepsin L, the angiogenic factors tissue factor (TF) and matrix metalloproteinase-9 (MMP-9), and the angiostatic factor tissue factor pathway inhibitor (TFPI) in proliferative diabetic retinopathy (PDR).

**Methods:** Vitreous samples from 25 patients with PDR and 20 nondiabetic patients and epiretinal membranes from 12 patients with PDR were studied with enzyme-linked immunosorbent assay, western blot analysis, and immunohistochemistry.

**Results:** We observed a significant increase in the expression of heparanase activity in vitreous samples from patients with PDR compared to the nondiabetic controls ( $p=0.027$ ). Significant positive correlations were found between the levels of heparanase activity and the levels of cathepsin L ( $r=0.51$ ;  $p=0.001$ ), TF ( $r=0.6$ ;  $p<0.0001$ ), and TFPI ( $r=0.49$ ;  $p=0.001$ ). The expression levels of cathepsin L ( $p=0.019$ ), TF ( $p<0.0001$ ), TFPI ( $p<0.0001$ ), and MMP-9 ( $p=0.029$ ) were significantly higher in the vitreous samples with detected heparanase activity compared to the vitreous samples with undetected heparanase activity. Western blot analysis demonstrated proteolytic cleavage of TFPI in the vitreous samples from patients with PDR. In the epiretinal membranes, cathepsin L, TF, and TFPI were expressed in vascular endothelial cells and CD45-expressing leukocytes. Significant positive correlations were detected between the number of blood vessels that expressed CD31 and the number of blood vessels that expressed TF ( $r=0.9$ ;  $p<0.0001$ ) and TFPI ( $r=0.81$ ;  $p=0.001$ ).

**Conclusions:** The coexpression of these angiogenesis regulatory factors suggests cross-talk between these factors and pathogenesis of PDR angiogenesis.

Ischemia-induced angiogenesis, the process by which new vascular networks develop from preexisting blood vessels, is the pathological hallmark in proliferative diabetic retinopathy (PDR) and often leads to catastrophic loss of vision due to vitreous hemorrhage and/or traction retinal detachment. Angiogenesis is a multistep process requiring the degradation of the basement membrane and the extracellular matrix (ECM), endothelial cell migration, endothelial cell proliferation, and capillary tube formation [1]. Angiogenesis is under tight regulation by a dynamic balance between angiogenic stimulators and inhibitors [2]. Vascular endothelial growth factor (VEGF) is the major angiogenic factor in PDR that promotes neovascularization and vascular

leakage [3]. Several studies have shown the overexpression of proinflammatory and proangiogenic factors in the ocular microenvironment of patients with PDR [4-8] suggesting that persistent inflammation and neovascularization are critical for PDR initiation and progression. Therapeutic regulation of angiogenesis has emerged as an attractive approach for the treatment of PDR [9]. To aid the progress of these strategies, a more comprehensive understanding of the molecules that regulate angiogenesis in PDR is of value to identify additional therapeutic targets and to avoid potential detrimental side effects.

Heparanase is an endo- $\beta$ -D-glucuronidase that cleaves heparan sulfate side chains of heparan sulfate proteoglycans on cell surfaces and in the basement membranes and the ECM, activity that is implicated in cell invasion associated with inflammation, angiogenesis, and tumor metastasis [10-18]. Human heparanase is initially produced as an

Correspondence to: Ahmed M. Abu El-Asrar, Department of Ophthalmology, King Abdulaziz University Hospital, Old Airport Road, P.O. Box 245, Riyadh 11411, Saudi Arabia; Phone: +966-11-4775723; FAX: +966-11-4775724; email: [abuasarar@KSU.edu.sa](mailto:abuasarar@KSU.edu.sa)

inactive proenzyme that undergoes post-translational processing to yield a secreted 65 kDa proenzyme. Proteolytic cleavage of proheparanase by the cysteine proteinase cathepsin L leads to the formation of catalytically active heparanase, a heterodimer consisting of a 50 kDa polypeptide non-covalently bound to an 8 kDa peptide [19]. Cathepsin L is found predominantly within the endosomal and lysosomal compartment of cells and is constitutively expressed in most tissues [20]. In our laboratory, we recently demonstrated that heparanase protein was upregulated in the vitreous fluid from patients with PDR and that heparanase protein was specifically localized in vascular endothelial cells and leukocytes in epiretinal fibrovascular membranes from patients with PDR [21]. Previous studies demonstrated active involvement of heparanase in the upregulation of the angiogenesis regulatory factors tissue factor (TF), tissue factor pathway inhibitor (TFPI), and matrix metalloproteinase-9 (MMP-9). In vitro and in vivo studies demonstrated that heparanase induces TF [22] and TFPI [23] expression in endothelial cells and cancer cells independent of heparanase enzymatic activity. The regulatory effect of heparanase of TF expression involved activation of the p38 signaling pathway [22]. Furthermore, elevation of heparanase expression in myeloma cells stimulates sustained extracellular signal-regulated kinase (ERK) phosphorylation that in turn drives MMP-9 expression. Heparanase enzymatic activity is required to enhance MMP-9 expression in these cells [24].

TF, a transmembrane glycoprotein present on the surface of most extravascular cells, is the primary initiator of coagulation. After vascular or endothelial injury, circulating factor (F) VII binds to the exposed TF receptor and undergoes proteolytic activation to become FVIIa. TF can also bind to FVIIa. This TF/FVIIa complex acts in concert with the anionic membrane phospholipid to convert circulating factors IX and X to IXa and Xa, respectively. FXa is the active catalytic component of the prothrombinase complex, which converts circulating prothrombin to thrombin. Thrombin in turn activates platelets and cleaves fibrinogen to produce an insoluble fibrin clot [25,26]. In recent years, a significant amount of evidence has demonstrated that TF and the TF/FVIIa complex can also promote angiogenesis, both directly and indirectly, through regulation of thrombin generation and activation of intracellular signaling mediated by protease-activated receptor-2 (PAR-2) [25-28].

TFPI is the major physiologic inhibitor of TF/FVIIa complex-mediated coagulation. TFPI is a multidomain serine protease inhibitor consisting of three independently folded Kunitz proteinase inhibitor (KPI) domains and a highly basic C-terminal tail [27]. The first KPI domain specifically

inhibits TF/FVIIa proteolytic activity, whereas the second KPI domain specifically inhibits FXa. TFPI inhibits coagulation by first blocking FXa activity and then forming a stable quaternary complex with TF/FVIIa complex [26]. Recent in vitro and in vivo models showed that TFPI has potent antitumor and antiangiogenesis activity independent of the potential effect of TFPI on TF [27,29-31].

The angiogenic switch involves in part the proteolytic degradation of basement membranes and ECM components by matrix metalloproteinases (MMPs). In PDR, the levels of MMP-9 are increased dramatically [8,32]. This upregulation of MMP-9 is linked to angiogenesis and progression of PDR. In addition, we demonstrated a significant positive correlation between the vitreous fluid levels of MMP-9 and VEGF [8]. MMP-9 may facilitate pathologic neovascularization through stimulation of the production of VEGF [33] and the proteolytic release of VEGF from the ECM-associated reservoirs [34,35], resulting in increased VEGF bioavailability and triggering the VEGF-driven angiogenic switch. MMP-9 has also been shown to be important in mobilizing endothelial and other progenitor cells from the bone marrow niche by releasing soluble kit ligand [36].

Although the role of heparanase, cathepsin L, TF, TFPI, and MMP-9 has become widely recognized in the regulation of angiogenesis, the correlation of the expression of these angiogenesis regulatory factors in PDR development is largely unknown. Therefore, we assayed heparanase enzymatic activity in the vitreous fluid from patients with PDR and correlated heparanase activity levels with the levels of cathepsin L, TF, TFPI, and MMP-9. In addition, we investigated the expression of cathepsin L, TF, and TFPI in epiretinal membranes from patients with PDR.

## METHODS

*Vitreous samples and epiretinal membranes specimens:* Undiluted vitreous fluid samples (0.3–0.6 ml) were obtained from 25 patients with PDR during pars plana vitrectomy. The indications for vitrectomy were tractional retinal detachment and/or nonclearing vitreous hemorrhage. The severity of retinal neovascular activity was graded clinically at the time of vitrectomy using previously published criteria [37]. Neovascularization was considered active if there were visible perfused new vessels on the retina or optic disc present within the epiretinal membranes. Neovascularization was considered inactive (involuting) if only nonvascularized, white fibrotic epiretinal membranes were present. Active PDR was present in 15 patients, and inactive PDR was present in 10 patients. Tractional retinal detachment was present in 16 patients and vitreous hemorrhage in 15 patients. The diabetic patients

were 13 men and 12 women, whose ages ranged from 25 to 76 years with a mean of  $54.6 \pm 12.7$  years. The control group consisted of 20 patients who had undergone vitrectomy for the treatment of rhegmatogenous retinal detachment with no proliferative vitreoretinopathy. Controls were free from systemic disease and were 13 men and seven women whose ages ranged from 33 to 71 years with a mean of  $47.1 \pm 17.4$  years. None of the control patients had vitreous hemorrhage. The ages ( $p=0.143$ ; Mann-Whitney test) and male/female ratios ( $p=0.38$ ; chi-square test) did not differ significantly between the nondiabetic control patients and the patients with PDR. Vitreous samples were collected undiluted by manual suction into a syringe through the aspiration line of vitrectomy, before the infusion line was opened. The samples were centrifuged ( $700 \times g$  for 10 min,  $4^\circ\text{C}$ ), and the supernatants were aliquoted and frozen at  $-80^\circ\text{C}$  until assay. Epiretinal fibrovascular membranes were obtained from 12 patients with PDR during pars plana vitrectomy for the repair of tractional retinal detachment. Membranes were fixed for 2 h in 10% formalin solution and embedded in paraffin.

The study was conducted according to the tenets of the Declaration of Helsinki. All patients were candidates for vitrectomy as a surgical procedure. All patients signed preoperative informed written consent and approved the use of the excised epiretinal membranes and vitreous fluid for further analysis and clinical research. The study design and the protocol were approved by the Research Centre and Institutional Review Board of the College of Medicine, King Saud University.

**Heparanase activity assay:** The quantitative measurement of heparanase enzymatic activity present in the vitreous fluid was performed using a heparan degrading assay kit (Cat No: MK412) purchased from Takara Bio Inc. (Shiga, Japan). This kit adapts a solid phase method using collagen binding domain-fibroblast growth factor domain (CBD-FGF) bound to a microtiter plate, a fusion protein of the cell-binding domain of human fibronectin and human basic fibroblast growth factor (bFGF). The kit is based on the method that when heparan sulfate is degraded by heparanase, heparan sulfate loses the ability to bind to bFGF. In addition, biotinylated heparan sulfate is used as a substrate for heparanase, and only undegraded substrate remains bound to CBD-FGF. The detection of the remaining undegraded substrate by avidin-peroxidase allows highly sensitive measurement of heparanase activity.

The protocol for quantification of heparanase activity was followed according to the manufacturer's instruction. The supplied reaction buffer contained protease inhibitors and glucuronidase inhibitors to minimize non-specific

degradation. A twofold dilution series of vitreous fluid samples was prepared with the reaction buffer. Similarly, a series of a standard enzyme preparation was made in reaction buffer. Undiluted enzyme standard served as the highest standard, and reaction buffer alone served as the zero standard. In a separate 96-well plate,  $50 \mu\text{l}$  of biotinylated heparan sulfate was incubated with the  $50 \mu\text{l}$  of all samples in reaction buffer. After incubation at  $37^\circ\text{C}$  for 45 min,  $90 \mu\text{l}$  of reactant was transferred to the wells of the CBD-FGF immobilized 96-well microtiter plate. Finally after washing and incubation with avidin peroxidase conjugate, the substrate was added. The reaction was stopped by adding stop solution (sulfuric acid). The heparanase activity was inversely correlated with absorbance measured at 450 nm for the undegraded biotinylated heparan sulfate bound to CBD-FGF with the avidin peroxidase conjugate. Each assay was performed in duplicate. Results were expressed in units per milliliter (u/ml) of vitreous fluid.

**Enzyme-linked immunosorbent assay:** Enzyme-linked immunosorbent assay (ELISA) kits for human MMP-9 (Cat No: ab100610), human cathepsin L (Cat No: ab119509), human TF (CD142, Cat No: ab108903), and TFPI (Cat No: ab108904) were purchased from Abcam (Cambridge, UK). The minimum detection limit for MMP-9, cathepsin L, TF, and TFPI was 10 pg/ml, 1.7 ng/ml, 4 pg/ml, and 0.1 ng/ml, respectively. The ELISA plate readings were performed using a Stat Fax-4200 microplate reader from Awareness Technology, Inc. (Palm City, FL). The quantification of human MMP-9, cathepsin L, TF, and TFPI in vitreous fluid was determined according to the manufacturer's instructions.

**Western blot analysis:** Western blot lysis buffer (30 mM Tris-HCl; pH 7.5, 5 mM EDTA, 1% Triton X-100, 250 mM sucrose, 1 mM Sodium vanadate, and protease inhibitor cocktail) was with protease inhibitor complete without EDTA (Roche, Mannheim, Germany). Equal volumes ( $15 \mu\text{l}$ ) of vitreous samples were boiled in Laemmli's sample buffer (1:1, v/v) under reducing conditions for 10 min and were subjected to sodium dodecyl sulfate-polyacrylamide gel (SDS-PAGE) electrophoresis in 10% gels and transferred onto nitrocellulose membranes (Bio-Rad Laboratories, Hercules, CA). Nonspecific binding sites were blocked (1.5 h, room temperature) with 5% non-fat milk made in Tris-buffered saline containing 0.1% Tween-20 [TBS-T]). Blots were then incubated at  $4^\circ\text{C}$  overnight using the following primary antibodies: anti-TF antibody (1:500; ab104513, Abcam) and anti-TFPI (1:500; ab180619, Abcam). Three TBS-T washings (5 min each) were performed before the respective secondary antibody treatment at room temperature for 1 h. Finally, the immunodetection was performed with the

use of chemiluminescence western blotting luminol reagent (sc-2048; Santa Cruz Biotechnology Inc., Santa Cruz, CA). Membranes were stripped and reprobed with  $\beta$ -actin-specific antibody (1:2,000; sc-47778; Santa Cruz Biotechnology Inc.) used as the lane-loading control. Bands were visualized with the use of a high-performance chemiluminescence machine (G: Box Chemi-XX8 from Syngene, Synoptic Ltd. Cambridge, UK), and the intensities were quantified by using GeneTools software (Syngene by Synoptic Ltd.).

**Immunohistochemical staining:** For CD31, antigen retrieval was performed by boiling the sections in citrate-based buffer (pH 5.9–6.1; BOND Epitope Retrieval Solution 1; Leica, Newcastle upon Tyne, UK) for 10 min. For cathepsin L, TF, TFPI, and CD45 detection, antigen retrieval was performed by boiling the sections in Tris/EDTA buffer (pH 9; BOND Epitope Retrieval Solution 2; Leica) for 20 min. Subsequently, the sections were incubated for 60 min with mouse monoclonal anti-CD31 (ready-to-use; clone JC70A; Dako, Glostrup, Denmark), mouse monoclonal anti-CD45 (ready-to-use; clones 2B11+PD7/26; Dako), mouse monoclonal anti-cathepsin L antibody (1:400; ab6314, Abcam), mouse monoclonal antibody against TF (1:50; ab17375, Abcam), and rabbit polyclonal antibody against human TFPI (1:200; ab180619, Abcam). Optimal working concentrations and incubation times for the antibodies were determined earlier in pilot experiments using sections from the kidney and patients with colon adenocarcinoma. The sections were then incubated for 20 min with a post-primary immunoglobulin G (IgG) linker followed by an alkaline phosphatase conjugated polymer. The reaction product was visualized by incubation for 15 min with the Fast Red chromogen (Dako Glostrup, Denmark), resulting in bright-red immunoreactive sites. The slides were then faintly counterstained with Mayer's hematoxylin (BOND Polymer Refine Red Detection Kit; Leica).

To identify the phenotype of cells that express TFPI and TF, sequential double immunohistochemistry was performed. The sections were incubated with the first primary antibody (anti-CD45) and subsequently treated with the peroxidase-conjugated secondary antibody. The sections were visualized with 3,3'-diaminobenzidine tetrahydrochloride. Incubation of the second primary antibody (anti-TFPI and anti-TF) was followed by treatment with the alkaline phosphatase-conjugated secondary antibody. The sections were visualized with Fast Red. No counterstain was applied. Omission or substitution of the primary antibody with an irrelevant antibody from the same species and staining with chromogen alone were used as negative controls.

**Quantitation:** Immunoreactive blood vessels and cells were counted in five representative fields, with the use of an

eyepiece-calibrated grid in combination with the 40X objective. These representative fields were selected based on the presence of immunoreactive blood vessels and cells. With this magnification and calibration, immunoreactive blood vessels and cells present in an area of 0.33 mm  $\times$  0.22 mm were counted.

**Statistical analysis:** Data are presented as the mean  $\pm$  standard deviation. The chi-square test and the non-parametric Mann–Whitney test were used to compare means from two independent groups. Pearson correlation coefficients were computed to investigate correlation between variables. A p value of less than 0.05 indicated statistical significance. SPSS version 20.0 for Windows (IBM Inc., Chicago, IL) was used for statistical analysis.

## RESULTS

**Heparanase enzymatic activity in vitreous samples:** Heparanase activity was detected in five of the 20 (25%) vitreous samples from the nondiabetic control patients and in 13 of the 25 (52%) vitreous samples from the patients with PDR. The mean heparanase enzymatic activity level in the vitreous samples from the patients with PDR (0.03 $\pm$ 0.07 u/ml) was significantly higher than that in the nondiabetic control patients (0.004 $\pm$ 0.009 u/ml; p=0.027; the Mann–Whitney test). When patients with PDR were divided into those with active neovascularization and those with quiescent disease, the mean levels of heparanase enzymatic activity in the vitreous samples from the patients with active PDR were significantly higher than in the patients with inactive PDR (p=0.01; Mann–Whitney test). The mean levels of heparanase enzymatic activity did not differ significantly between the patients with PDR with hemorrhage and the patients with PDR without hemorrhage and between the patients with PDR with or without tractional retinal detachment (Table 1).

**TABLE 1. COMPARISONS OF MEAN  $\pm$ SD LEVELS OF HEPARANASE ENZYMATIC ACTIVITY IN VITREOUS FLUID SAMPLES ACCORDING TO TYPE OF PROLIFERATIVE DIABETIC RETINOPATHY (PDR).**

Disease group	Heparanase activity ( $\mu$ /ml)	p value
- Active PDR (n=15)	0.056 $\pm$ 0.078	0.01*
- Inactive PDR (n=10)	0.0071 $\pm$ 0.0167	
- PDR with hemorrhage (n=15)	0.044 $\pm$ 0.071	0.119
- PDR without hemorrhage (n=10)	0.025 $\pm$ 0.058	
- PDR with TRD (n=16)	0.026 $\pm$ 0.049	0.141
- PDR without TRD (n=9)	0.054 $\pm$ 0.088	

\*Statistically significant at 5% level of significance. TRD=tractional retinal detachment.

*ELISA levels of cathepsin L, TF, TFPI, and MMP-9 in vitreous samples:* With the use of ELISA, we demonstrated that cathepsin L was detected in all vitreous samples from the patients with PDR and the nondiabetic control patients. The mean levels of cathepsin L did not differ significantly between the nondiabetic control patients (2.8±1.7 ng/ml) and the patients with PDR (2.5±1.1 ng/ml; p=0.7; the Mann–Whitney test).

TF was detected in six of the 20 (30%) vitreous samples from the nondiabetic control patients and in 14 of the 25 (56%) vitreous samples from the patients with PDR. The mean TF levels in the vitreous samples from the patients with PDR (23.3±35.9 pg/ml) were higher than those in the nondiabetic control patients (11.8±22.2 pg/ml); however, the difference was not statistically significant (p=0.095; the Mann–Whitney test).

TFPI was detected in all vitreous samples from the patients with PDR and the nondiabetic control patients. The mean TFPI level in the vitreous samples from the patients with PDR (13.5±4.0 pg/ml) was significantly higher than the mean level in the nondiabetic control patients (6.0±2.9 pg/ml; p<0.0001; the Mann–Whitney test).

MMP-9 was detected in all vitreous samples from the patients with PDR and the nondiabetic control patients. The mean MMP-9 level in the vitreous samples from the patients with PDR (4.5±5.5 ng/ml) was significantly higher than the mean level in the nondiabetic control patients (0.75±0.6 ng/ml; p<0.0001; the Mann–Whitney test).

*Correlations:* Significant positive correlations were found between the vitreous fluid levels of heparanase enzymatic activity and the levels of cathepsin L, TF, and TFPI. There were significant positive correlations between the vitreous fluid levels of cathepsin L and the levels of TF and TFPI. A positive significant correlation was observed between the TF and TFPI vitreous levels and between the MMP-9 and TFPI vitreous levels (Table 2).

*Relationship between detection of heparanase enzymatic activity and the levels of cathepsin L, TF, TFPI, and MMP-9 in vitreous fluid samples:* The entire study group was divided into those with detected heparanase enzymatic activity in vitreous fluid samples and those without detectable heparanase enzymatic activity. The mean levels of cathepsin L, TF, TFPI, and MMP-9 in vitreous fluid samples with detected heparanase enzymatic activity were significantly higher than those in vitreous fluid samples with undetectable heparanase enzymatic activity (Table 3).

*Western blot analysis of vitreous samples:* With the use of western blot analysis of equal volumes (15 µl) of vitreous

TABLE 2. PEARSON CORRELATION COEFFICIENTS.

Variable	Coefficient				
	P value	Hepa-ranase activity	Cathepsin L	TF	TFPI
Cathepsin L	r	0.51*			
	p	0.001			
TF	r	0.6*	0.6*		
	p	<0.0001	<0.0001		
TFPI	r	0.49*	0.49*	0.58*	
	p	0.001	0.001	<0.0001	
MMP-9	r	0.09	0.22	-0.01	0.42*
	p	0.533	0.164	0.941	0.005

\*Statistically significant at 5% level of significance. Where the row and column meet is the correlation coefficient and the p value for the two variables. TF=tissue factor; TFPI=tissue factor pathway inhibitor; MMP-9=matrix metalloproteinase-9

samples, we confirmed that TF and TFPI were expressed in the vitreous samples. Densitometric analysis of the bands showed a significant increase in TF expression in the vitreous samples from the patients with PDR (n=12) compared to the vitreous samples from the nondiabetic control patients (n=12; Figure 1A; p=0.0001; Mann-Whitney test). In the vitreous samples, the TFPI protein migrated as two protein bands on SDS–PAGE when immunoblotted and analyzed with the specific antibody. The upper band corresponded to the intact protein (around 50 kDa), whereas the lower protein band corresponded to the cleaved TFPI (around 22 kDa). Densitometric analysis of the bands demonstrated that the intact TFPI (p=0.0001; Mann-Whitney test) and the cleaved TFPI (p=0.01; Mann-Whitney test) were significantly higher in the vitreous samples from the patients with PDR compared to

TABLE 3. COMPARISONS OF MEAN ± SD LEVELS OF CATHEPSIN L, TF, TFPI AND MMP-9 IN VITREOUS FLUID SAMPLES ACCORDING TO DETECTION OF HEPARANASE ENZYMATIC ACTIVITY.

Variable	Heparanase activity detected	Heparanase activity undetected	P value
Cathepsin L (ng/ml)	3.5±2.1	2.2±0.8	0.019*
TF (pg/ml)	45.9±40.1	5.1±9.3	<0.0001*
TFPI (pg/ml)	14.8±3.9	8.1±4.1	<0.0001*
MMP-9 (ng/ml)	4.4±5.6	1.1±1.0	0.029*

\*Statistically significant at 5% level of significance. TF=tissue factor; TFPI=tissue factor pathway inhibitor; MMP-9=matrix metalloproteinase-9

the vitreous samples from the nondiabetic control patients (Figure 1B).

**Immunohistochemical analysis of epiretinal membranes:** To identify possible sources of vitreous fluid cathepsin L, TF, and TFPI, epiretinal fibrovascular membranes from patients with PDR were studied with immunohistochemical analysis. No staining was observed in the negative control slides (Figure 2A). The level of vascularization and proliferative activity in the epiretinal membranes were determined by immunodetection of the endothelial cell marker CD31. All membranes showed blood vessels that were positive for the endothelial cell marker CD31 (Figure 2B) with a mean

of  $51.8 \pm 24.1$  (range 25–95). Strong widespread immunoreactivity for cathepsin L was present in all membranes and was noted in vascular endothelial cells and stromal cells (Figure 2C,D). Immunoreactivity for TF was present in all membranes and was noted in vascular endothelial cells and stromal cells (Figure 3A). The number of blood vessels that were immunoreactive for TF ranged from 15 to 80, with a mean of  $32.1 \pm 22.7$ . The number of TF-positive stromal cells ranged from 20 to 75, with a mean of  $27.0 \pm 19.9$ . Strong immunoreactivity for TFPI was present in all membranes and was noted in vascular endothelial cells, stromal cells, and intravascular leukocytes (Figure 3B,C). The number of

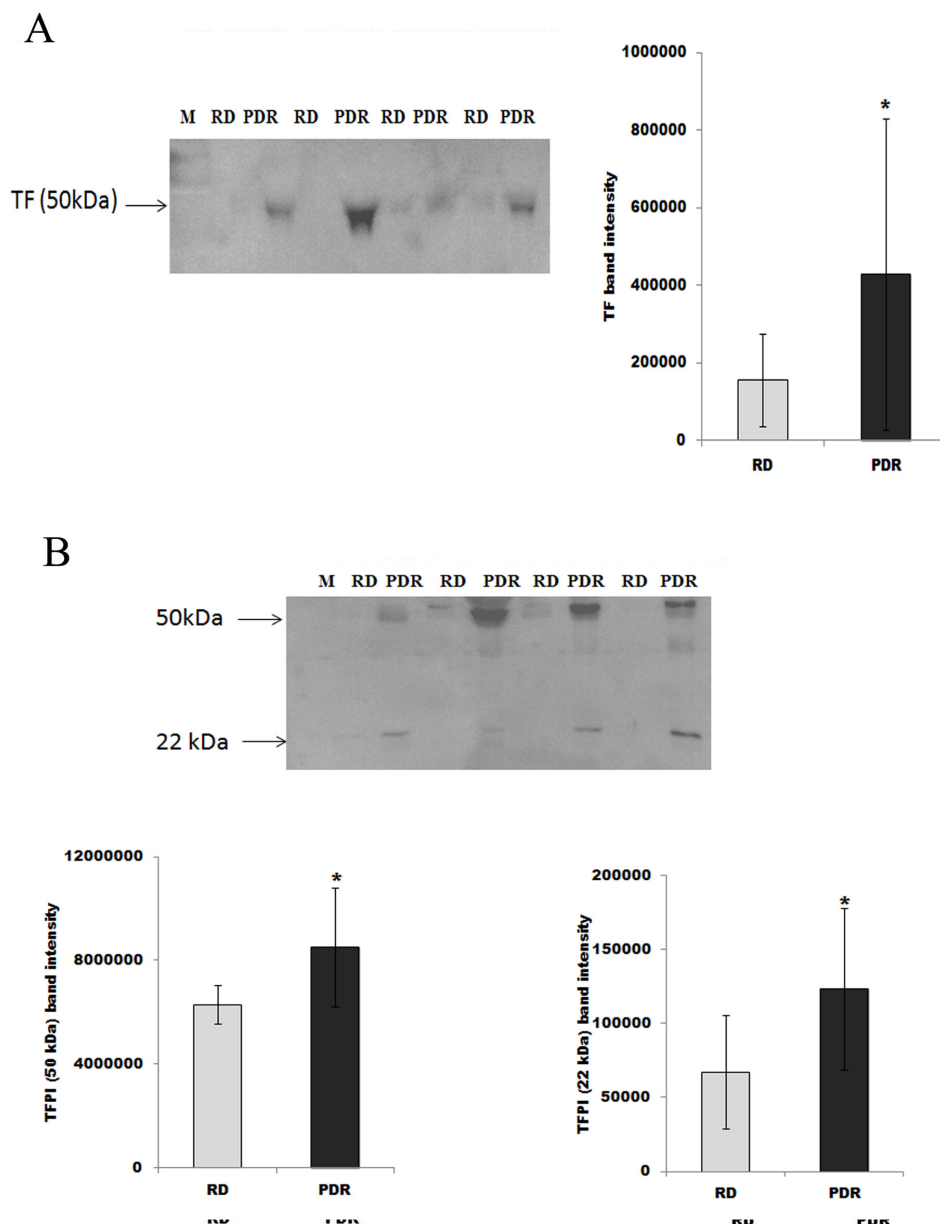


Figure 1. The expression levels of tissue factor (TF) and tissue factor pathway inhibitor (TFPI) in equal volumes (15  $\mu$ l) of vitreous fluid samples obtained from patients with proliferative diabetic retinopathy (PDR; n=12) and from control patients without diabetes (RD; n=12) were determined with Western blot analysis. A representative set of samples is shown. The resultant data are presented in the histograms as mean  $\pm$  standard deviation. The expressions of TF (A) and both intact and cleaved TFPI (B) are significantly increased in vitreous samples from PDR patients compared to control patients without diabetes. \*The difference between the two means was statistically significant at the 5% level of significance (p=0.0001; p=0.0001; p=0.01, respectively; Mann-Whitney test).

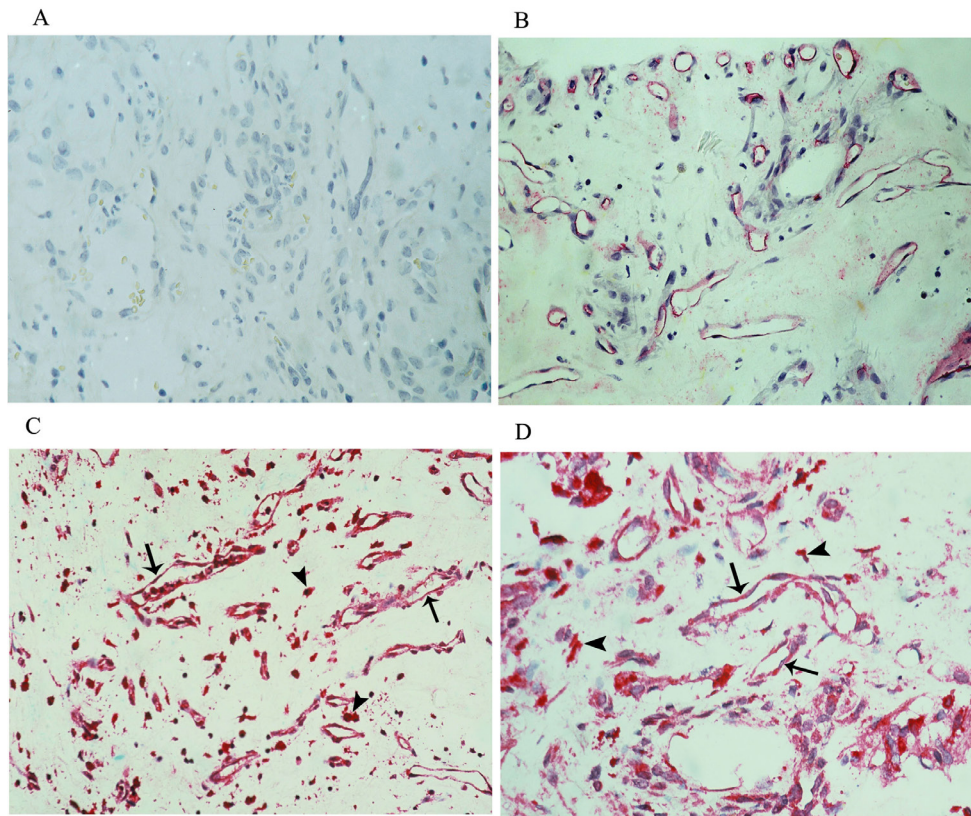


Figure 2. Proliferative diabetic retinopathy epiretinal membranes. **A:** A negative control slide that was treated with an irrelevant antibody showed no labeling (original magnification 40X). **B:** Immunohistochemical staining for CD31 showing blood vessels positive for CD31 (original magnification 40X). Immunohistochemical staining for cathepsin L showing immunoreactivity in vascular endothelial cells (arrows) and stromal cells (arrowheads). **C:** Low power (original magnification 25X). **D:** High power (original magnification 40X).

blood vessels that were immunoreactive for TFPI ranged from 30 to 75, with a mean of  $48.8 \pm 17.1$ . The number of stromal cells that were immunoreactive for TFPI ranged from 35 to 75, with a mean of  $44.6 \pm 22.8$ . In the serial sections, the distribution and morphologies of stromal cells that expressed TF and TFPI were similar to those of the cells that expressed the leukocyte common antigen CD45 (Figure 4A,B). Double staining confirmed that the stromal cells and intravascular leukocytes that expressed TF and TFPI coexpressed CD45 (Figure 4C,D). Significant positive correlations were detected between the number of blood vessels that expressed CD31 and the number of blood vessels that expressed TF ( $r=0.9$ ;  $p<0.0001$ ) and TFPI ( $r=0.81$ ;  $p=0.001$ ).

## DISCUSSION

The angiogenic potency of heparanase has been confirmed in several *in vitro* and *in vivo* model systems providing a strong clinical evidence for the proangiogenic function of heparanase [10,12,14,16,38,39]. Heparanase upregulation correlates with microvessel density in various primary human tumors [10,12]. In our laboratory, using immunohistochemistry, we demonstrated a significant positive correlation between the level of vascularization in PDR epiretinal membranes and the number of blood vessels and stromal cells that express heparanase

protein. In addition, we found a significant positive correlation between the vitreous fluid levels of the heparanase protein and those of the angiogenic biomarker VEGF [21]. In the present study, the vitreous levels of heparanase enzymatic activity were higher in the PDR eyes with active neovascularization compared with the eyes with quiescent disease. This effect of heparanase on angiogenesis is thought to be mediated by several mechanisms. Heparanase enzymatic activity has been associated with destruction of the basement membrane before cell invasion, an event that may enhance endothelial cell migration. Heparanase can also release heparan sulfate-bound growth factors such as VEGF. In addition, heparanase stimulates shedding of the transmembrane heparan sulfate proteoglycan syndecan-1 from the cell surface induced by the enzymatic activity of heparanase stimulation. VEGF forms a complex with the shed syndecan-1 that can bind to the ECM and subsequently activates VEGF receptors on adjacent endothelial cells leading to enhanced endothelial cell invasion and angiogenesis [10,12,14,24,38,40,41]. Shed syndecan-1 in addition to presenting VEGF to endothelial cells can also activate  $\alpha\beta3$  integrin, a key regulator of endothelial cell activation and angiogenesis [41]. Furthermore, via nonenzymatic activity, heparanase can stimulate upregulation of VEGF, activation of intracellular signaling

molecules, and endothelial cell invasion and migration, key early steps in angiogenesis [16,42]. Heparanase enzymatic activity was detected in 25% of the vitreous samples from patients with rhegmatogenous retinal detachment with no proliferative vitreoretinopathy. These findings are consistent with previous reports that demonstrated upregulated expression of inflammatory mediators in the vitreous fluid from patients with rhegmatogenous retinal detachment [43-45] and in the detached retina following experimental retinal detachment [46]. In addition, we recently demonstrated that heparanase protein was detected in 22.2% of vitreous samples from patients with rhegmatogenous retinal detachment with no proliferative vitreoretinopathy [21].

In the present study, we detected the simultaneous expression of heparanase enzymatic activity, cathepsin L, TF, TFPI, and MMP-9 in the vitreous fluid from patients with PDR. There were significant positive correlations between the levels of heparanase enzymatic activity and the levels of cathepsin L, TF, and TFPI. Furthermore, the mean cathepsin L, TF, TFPI, and MMP-9 levels in vitreous fluid samples with detected heparanase enzymatic activity were significantly higher than those in the vitreous fluid samples without detectable heparanase enzymatic activity. These findings are in accordance with previous reports that demonstrated active

involvement of heparanase in the upregulation of TF [22], TFPI [23], and MMP-9 [24]. In previous studies, we demonstrated MMP-9 [8] and heparanase protein [21] localization in vascular endothelial cells and leukocytes in epiretinal fibrovascular membranes from patients with PDR. Similarly, in the present study, cathepsin L, TF, and TFPI were specifically localized in vascular endothelial cells and leukocytes in PDR epiretinal membranes. The coexpression of these angiogenesis regulatory factors in the ocular microenvironment of patients with PDR suggests cross-talk between these factors in the pathogenesis of PDR angiogenesis and progression and that the coexpression of these factors is mechanistically interrelated.

TF, the most potent initiator of coagulation, is expressed aberrantly in many types of malignancy and is involved not only in tumor-associated hypercoagulability but also in promoting tumor angiogenesis, growth, and metastasis [25-28,47]. Ample evidence exists that TF expression in solid tumors is an independent predictor of poor overall or relapse-free survival [26,28]. TF expression in tumor cells correlates with the microvessel density and the ability of tumors to secrete VEGF and consequently induces an angiogenic response [26,28,47,48]. Although TF is not normally expressed on endothelial cells, using immunohistochemistry,

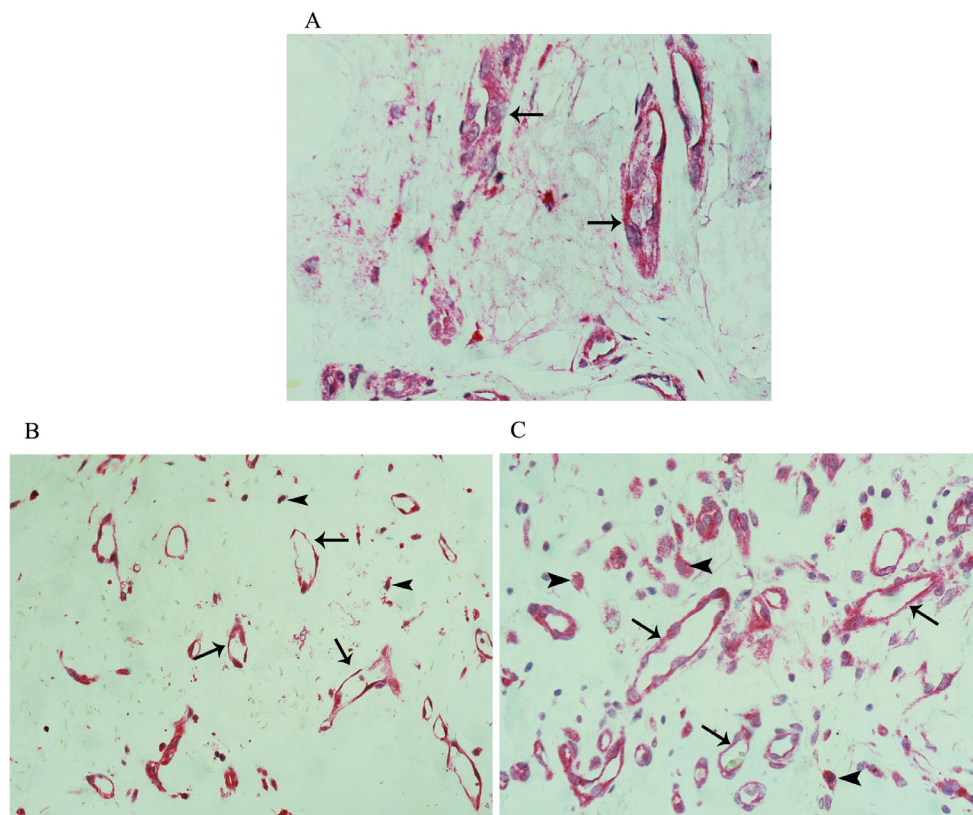


Figure 3. Proliferative diabetic retinopathy epiretinal membranes. **A:** Immunohistochemical staining for tissue factor showing immunoreactivity in vascular endothelial cells (original magnification 40X). Immunohistochemical staining for tissue factor pathway inhibitor showing immunoreactivity in vascular endothelial cells (arrows) and stromal cells (arrowheads). **B:** Low power (original magnification 25X). **C:** High power (original magnification 40X).

we demonstrated that the TF protein was localized in vascular endothelial cells and leukocytes in the epiretinal fibrovascular membranes from the patients with PDR. Similarly, TF is upregulated on endothelial cells within breast cancer [49] and retinoblastoma [50], and elevated levels of TF are correlated with an invasive carcinoma phenotype [49] and has been proposed to enhance angiogenesis [26,28].

In vivo and in vitro data showed that TFPI has potent antiangiogenesis activity [29-31,50]. TFPI specifically inhibits vascular endothelial cell migration and tube formation induced by basic fibroblast growth factor [29], fibroblast growth factor-2 [50], and VEGF [31]. In addition, TFPI directly blocks VEGF receptor 2 activation [31]. In vitro studies suggest that the interaction of TFPI with the very low density lipoprotein (VLDL) receptor is part of the mechanisms mediating its antiangiogenic and antitumor roles [30]. In the present study, we showed that TFPI was specifically localized in vascular endothelial cells and leukocytes in the epiretinal fibrovascular membranes from the patients with PDR and that there was a significant positive correlation between the level of vascularization in the PDR epiretinal membranes and the number of blood vessels that express TFPI. Our data are in line with those from others who have shown that TFPI levels are elevated in advanced cancer [25]

and that TFPI is expressed by endothelial cells of small blood vessels and tumor-infiltrating macrophages in several human tumors [51]. Data from animal studies suggest that vascular expression of TFPI inhibits pathologic vascular remodeling and inhibits angiogenesis [27]. Our findings suggest that the upregulation of TFPI in PDR and the presence of a significant positive correlation between its levels and the levels of the angiogenic stimulators' heparanase enzymatic activity, TF and MMP-9, may be a protective antiangiogenesis eye response to suppress progression of PDR through inhibiting retinal angiogenesis.

In the present study, western blot analysis demonstrated the presence of intact (around 50 kDa) and cleaved (around 22 kDa) TFPI in the vitreous fluid from patients with PDR and that both products were increased in the vitreous samples from the patients with PDR. These findings are consistent with a previous study that demonstrated the matrix metalloproteinases MMP-1, MMP-7, MMP-9, and MMP-12 cleave TFPI into several fragments [52]. In a previous study, we demonstrated upregulation of MMP-1, MMP-7, and MMP-9 in vitreous samples from patients with PDR [8]. The rates of cleavage were most rapid for MMP-7 and MMP-9 [52]. In contrast, these MMPs did not cleave TF. Proteolytic cleavage of TFPI results in considerable loss of TFPI biologic activity

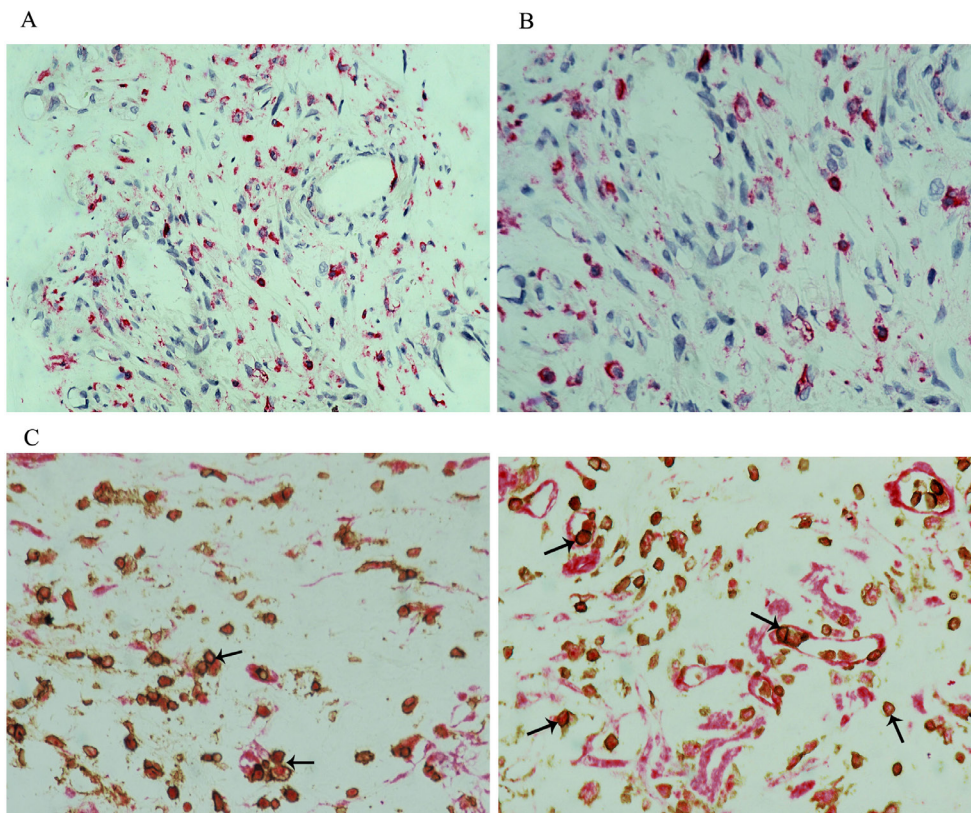


Figure 4. Proliferative diabetic retinopathy epiretinal membranes. Immunohistochemical staining for CD45. **A:** Low power (original magnification 25X). **B:** High power (original magnification 40X). Double immunohistochemistry for CD45 (brown) and tissue factor pathway inhibitor (TFPI; red) showing stromal cells and intravascular leukocytes (arrows) coexpressing CD45 and TFPI (C and D; original magnification 40X).

[52]. The present findings suggest that overexpression of MMP-9 in PDR reduces the TFPI endogenous protective system and thus enhances the angiogenic switch and allows the progression of PDR angiogenesis. The positive correlation between MMP-9 and TFPI expression suggests the possible mechanism of coordinated action of MMP-9 and TFPI.

In conclusion, the findings suggest a potential link between heparanase enzymatic activity, cathepsin L, TF, TFPI, and MMP-9 in the pathogenesis of PDR. The upregulation of TFPI may be a protective antiangiogenesis eye response to suppress progression of PDR, which is apparently not potent enough due to its proteolytic cleavage by enzymes, such as MMP-9.

### ACKNOWLEDGMENTS

The authors thank Ms. Kathleen van den Eynde, Mr. Wilfried Versin and Ms. Nathalie Volders for technical assistance and Ms. Connie Unisa-Marfil for secretarial work. This work was supported by Dr. Nasser Al-Rashid Research Chair in Ophthalmology (Abu El-Asrar AM),

### REFERENCES

- Deryugina EI, Quigley JP. Pleiotropic roles of matrix metalloproteinases in tumor angiogenesis: contrasting, overlapping and compensatory functions. *Biochim Biophys Acta* 2010; xxx:103-20. .
- Hanahan D, Folkman J. Patterns and emerging mechanisms of the angiogenic switch during tumorigenesis. *Cell* 1996; 86:353-64. [PMID: 8756718].
- Spranger J, Pfeiffer AF. New concepts in pathogenesis and treatment of diabetic retinopathy. *Exp Clin Endocrinol Diabetes* 2001; 109:Suppl 2S438-50. [PMID: 11460590].
- Abu El-Asrar AM, Nawaz MI, De Hertogh G, Alam K, Siddiquei MM, Van den Eynde K, Mousa A, Mohammad G, Geboes K, Opdenakker G. S100A4 is upregulated in proliferative diabetic retinopathy and correlates with markers of angiogenesis and fibrogenesis. *Mol Vis* 2014; 20:1209-24. [PMID: 25253987].
- Abu El-Asrar AM, Nawaz MI, Kangave D, Siddiquei MM, Geboes K. Angiogenic and vasculogenic factors in the vitreous from patients with proliferative diabetic retinopathy. *J Diabetes Res* 2013; 539658:[PMID: 23671874].
- El-Asrar AM, Nawaz MI, Kangave D, Geboes K, Ola MS, Ahmad S, Al-Shabrawey M. High-mobility group box-1 and biomarkers of inflammation in the vitreous from patients with proliferative diabetic retinopathy. *Mol Vis* 2011; 17:1829-38. [PMID: 21850157].
- Nawaz MI, Van Raemdonck K, Mohammad G, Kangave D, Van Damme J, Abu El-Asrar AM, Struyf S. Autocrine CCL2, CXCL4, CXCL9 and CXCL10 signal in retinal endothelial cells and are enhanced in diabetic retinopathy. *Exp Eye Res* 2013; 109:67-76. [PMID: 23352833].
- Abu El-Asrar AM, Mohammad G, Nawaz MI, Siddiquei MM, Van den Eynde K, Mousa A, De Hertogh G, Opdenakker G. Relationship between vitreous levels of matrix metalloproteinases and vascular endothelial growth factor in proliferative diabetic retinopathy. *PLoS One* 2013; 8:e85857-[PMID: 24392031].
- Salam A, Mathew R, Sivaprasad S. Treatment of proliferative diabetic retinopathy with anti-VEGF agents. *Acta Ophthalmol* 2011; 89:405-11. [PMID: 21294854].
- Nadir Y, Brenner B. Heparanase multiple effects in cancer. *Thromb Res* 2014; 133:Suppl 2S90-4. [PMID: 24862152].
- Simeonovic CJ, Ziolkowski AF, Wu Z, Choong FJ, Freeman C, Parish CR. Heparanase and autoimmune diabetes. *Front Immunol* 2013; 4:471-[PMID: 24421779].
- Vlodavsky I, Beckhove P, Lerner I, Pisano C, Meirovitz A, Ilan N, Elkin M. Significance of heparanase in cancer and inflammation. *Cancer Microenviron* 2012; •••:115-32. [PMID: 21811836].
- Goldberg R, Meirovitz A, Hirshoren N, Bulvik R, Binder A, Rubinstein AM, Elkin M. Versatile role of heparanase in inflammation. *Matrix Biol* 2013; 32:234-40. [PMID: 23499528].
- Meirovitz A, Goldberg R, Binder A, Rubinstein AM, Hermanto E, Elkin M. Heparanase in inflammation and inflammation-associated cancer. *FEBS J* 2013; 280:2307-19. [PMID: 23398975].
- Inatani M, Tanihara H. Proteoglycans in retina. *Prog Retin Eye Res* 2002; 21:429-47. [PMID: 12207944].
- Zetser A, Bashenko Y, Edovitsky E, Levy-Adam F, Vlodavsky I, Ilan N. Heparanase induces vascular endothelial growth factor expression: correlation with p38 phosphorylation levels and Src activation. *Cancer Res* 2006; 66:1455-63. [PMID: 16452201].
- Edovitsky E, Lerner I, Zcharia E, Peretz T, Vlodavsky I, Elkin M. Role of endothelial heparanase in delayed-type hypersensitivity. *Blood* 2006; 107:3609-16. [PMID: 16384929].
- Lever R, Rose MJ, McKenzie EA, Page CP. Heparanase induces inflammatory cell recruitment in vivo by promoting adhesion to vascular endothelium. *Am J Physiol Cell Physiol* 2014; 306:C1184-90. [PMID: 24740543].
- Abboud-Jarrou G, Atzmon R, Peretz T, Palermo C, Gadea BB, Joyce JA, Vlodavsky I. Cathepsin L is responsible for processing and activation of proheparanase through multiple cleavages of a linker segment. *J Biol Chem* 2008; 283:18167-76. [PMID: 18450756].
- Reiser J, Adair B, Reinheckel T. Specialized roles for cysteine cathepsin in health and disease. *J Clin Invest* 2010; 120:3421-31. [PMID: 20921628].
- Abu El-Asrar AM, Alam K, Nawaz MI, Mohammad G, Van den Eynde K, Siddiquei MM, Mousa A, De Hertogh G, Geboes K, Opdenakker G. Upregulated expression of heparanase in the vitreous of patients with proliferative diabetic

- retinopathy originates from activated endothelial cells and leukocytes. *Invest Ophthalmol Vis Sci* 2015; 56:8239-47. [PMID: 26720478].
22. Nadir Y, Brenner B, Zetser A, Ilan N, Shafat I, Zcharia E, Goldshmidt O, Vlodaysky I. Heparanase induces tissue factor expression in vascular endothelial and cancer cells. *J Thromb Haemost* 2006; 4:2443-51. [PMID: 16970801].
  23. Nadir Y, Brenner B, Gingis-Velitski S, Levy-Adam F, Ilan N, Zcharia E, Nadir E, Vlodaysky I. Heparanase induces tissue factor pathway inhibitor expression and extracellular accumulation in endothelial and tumor cells. *Thromb Haemost* 2008; 99:133-41. [PMID: 18217145].
  24. Purushothaman A, Chen L, Yang Y, Sanderson RD. Heparanase stimulation of protease expression implicates it as a master regulator of the aggressive tumor phenotype in myeloma. *J Biol Chem* 2008; 283:32628-36. [PMID: 18812315].
  25. Amirkhosravi A, Meyer T, Amaya M, Davila M, Mousa SA, Robson T, Francis JL. The role of tissue factor pathway inhibitor in tumor growth and metastasis. *Semin Thromb Hemost* 2007; 33:643-52. [PMID: 18000790].
  26. van den Berg YW, Osanto S, Reitsma PH, Versteeg HH. The relationship between tissue factor and cancer progression: insights from bench and bedside. *Blood* 2012; 119:924-32. [PMID: 22065595].
  27. Holroyd EW, White TA, Pan S, Simari RD. Tissue factor pathway inhibitor as a multifunctional mediator of vascular structure. *Front Biosci (Elite Ed)* 2012; 4:392-400. [PMID: 22201881].
  28. Kasthuri RS, Taubman MB, Mackman N. Role of tissue factor in cancer. *J Clin Oncol* 2009; 27:4834-8. [PMID: 19738116].
  29. Hembrough TA, Ruiz JF, Papatianassiu AE, Green SJ, Strickland DK. Tissue factor pathway inhibitor inhibits endothelial cell proliferation via association with the very low density lipoprotein receptor. *J Biol Chem* 2001; 276:12241-8. [PMID: 11278667].
  30. Hembrough TA, Ruiz JF, Swerdlow BM, Swartz GM, Hammers HJ, Zhang L, Plum SM, Williams MS, Strickland DK, Pribluda VS. Identification and characterization of a very low density lipoprotein receptor-binding peptide from tissue factor pathway inhibitor that has antitumor and antiangiogenic activity. *Blood* 2004; 103:3374-80. [PMID: 14739228].
  31. Holroyd EW, Delacroix S, Larsen K, Harbuzariu A, Psaltis PJ, Wang L, Pan S, White TA, Witt TA, Kleppe LS, Mueske CS, Mukhopadhyay D, Simari RD. Tissue factor pathway inhibitor blocks angiogenesis via its carboxyl terminus. *Arterioscler Thromb Vasc Biol* 2012; 32:704-11. [PMID: 2223730].
  32. Descamps FJ, Martens E, Kangave D, Struyf S, Geboes K, Van Damme J, Opdenakker G, Abu El-Asrar AM. The activated form of gelatinase B/matrix metalloproteinase-9 is associated with diabetic vitreous hemorrhage. *Exp Eye Res* 2006; 83:401-7. [PMID: 16643893].
  33. Hollborn M, Stathopoulos C, Steffen A, Wiedemann P, Kohlen L, Bringmann A. Positive feedback regulation between MMP-9 and VEGF in human RPE cells. *Invest Ophthalmol Vis Sci* 2007; 48:4360-7. [PMID: 17724228].
  34. Hawinkels LJ, Zuidwijk K, Verspaget HW, de Jonge-Muller ES, van Duijn W, Ferreira V, Fontijn RD, David G, Hommes DW, Lamers CB, Sier CF. VEGF release by MMP-9 mediated heparan sulphate cleavage induces colorectal cancer angiogenesis. *Eur J Cancer* 2008; 44:1904-13. [PMID: 18691882].
  35. Ebrahem Q, Chaurasia SS, Vasani A, Qi JH, Klenotic PA, Cutler, Asosingh K, Erzurum S, Anand-Apte B. Cross-talk between vascular endothelial growth factor and matrix metalloproteinases in the induction of neovascularization in vivo. *Am J Pathol* 2010; 176:496-503. [PMID: 19948826].
  36. Heissig B, Hattori K, Dias S, Friedrich M, Ferris B, Hackett NR, Crystal RG, Besmer P, Lyden D, Moore MA, Werb Z, Rafii S. Recruitment of stem and progenitor cells from the bone marrow niche requires MMP-9 mediated release of kit-ligand. *Cell* 2002; 109:625-37. [PMID: 12062105].
  37. Aiello LP, Avery RL, Arrigg PG, Keyt BA, Jampel HD, Shah ST, Pasquale LR, Thieme H, Iwamoto MA, Park JE, Nguyen HV, Aiello LM, Ferrara N, King GL. Vascular endothelial growth factor in ocular fluid of patients with diabetic retinopathy and other retinal disorders. *N Engl J Med* 1994; 331:1480-7. [PMID: 7526212].
  38. Yang Y, Macleod V, Miao HQ, Theus A, Zhan F, Shaughnessy JD Jr, Sawyer J, Li JP, Zcharia E, Vlodaysky I, Sanderson RD. Heparanase enhances syndecan-1 shedding: a novel mechanism for stimulation of tumor growth and metastasis. *J Biol Chem* 2007; 282:13326-33. [PMID: 17347152].
  39. Luan Q, Sun J, Li C, Zhang G, Lv Y, Wang G, Li C, Ma C, Gao T. Mutual enhancement between heparanase and vascular endothelial growth factor: a novel mechanism for melanoma progression. *Cancer Lett* 2011; 308:100-11. [PMID: 21624769].
  40. Purushothaman A, Uyama T, Kobayashi F, Yamada S, Sugahara K, Rapraeger AC, Sanderson RD. Heparanase-enhanced shedding of syndecan-1 by myeloma cells promotes endothelial invasion and angiogenesis. *Blood* 2010; 115:2449-57. [PMID: 20097882].
  41. Ramani VC, Purushothaman A, Stewart MD, Thompson CA, Vlodaysky I, Au JL, Sanderson RD. The heparanase/syndecan-1 axis in cancer: mechanisms and therapies. *FEBS J* 2013; 280:2294-306. [PMID: 23374281].
  42. Gingis Velitski S, Zetser A, Flugelman MY, Vlodaysky I, Ilan N. Heparanase induces endothelial cell migration via protein kinase B/Akt activation. *J Biol Chem* 2004; 279:23536-41. [PMID: 15044433].
  43. Dai Y, Wu Z, Sheng H, Yu M, Zhang Q. Identification of inflammatory mediators in patients with rhegmatogenous retinal detachment associated with choroidal detachment. *Mol Vis* 2015; 21:417-27. [PMID: 26015767].
  44. Yoshimura T, Sonoda KH, Sugahara M, Mochizuki Y, Enaida H, Oshima Y, Ueno a, Hata Y, Yoshida H, Ishibashi T. Comprehensive analysis of inflammatory immune mediators

- in vitreoretinal diseases. *PLoS One* 2009; 4:e8158-[\[PMID: 19997642\]](#).
45. Abu El-Asrar AM, Van Damme J, Put W, Veckeneer M, Dralands L, Billiau A, Missotten L. Monocyte chemotactic protein-1 in proliferative vitreoretinal disorders. *Am J Ophthalmol* 1997; 123:599-606. [\[PMID: 9152065\]](#).
  46. Nakazawa T, Matsubara A, Noda K, Hisatomi T, She H, Skondra D, Mihahara S, Sobrin L, Thomas KL, Chen DF, Grosskreutz CL, Hafezi-Moghadam A, Miller JW. Characterization of cytokine responses to retinal detachment in rats. *Mol Vis* 2006; 12:867-78. [\[PMID: 16917487\]](#).
  47. Chen J, Bierhaus A, Schiekofer S, Andrassy M, Chen B, Stern DM, Nawroth PP. Tissue factor—a receptor involved in the control of cellular properties, including angiogenesis. *Thromb Haemost* 2001; 86:334-45. [\[PMID: 11487022\]](#).
  48. Zhang Y, Deng Y, Luther T, Müller M, Ziegler R, Waldherr R, Stern DM, Nawroth PP. Tissue factor controls the balance of angiogenic and antiangiogenic properties of tumor cells in mice. *J Clin Invest* 1994; 94:1320-7. [\[PMID: 7521887\]](#).
  49. Contrino J, Hair G, Kreutzer DL, Rickles FR. In situ detection of tissue factor in vascular endothelial cells: correlation with the malignant phenotype of human breast disease. *Nat Med* 1996; 2:209-15. [\[PMID: 8574967\]](#).
  50. Song HB, Park KD, Kim JH, Kim DH, Yu YS, Kim JH. Tissue factor regulated tumor angiogenesis of retinoblastoma via the extracellular signal-regulated kinase pathway. *Oncol Rep* 2012; 28:2057-62. [\[PMID: 23007470\]](#).
  51. Sierko E, Wojtukiewicz MZ, Zimnoch L, Kisiel W. Expression of tissue factor pathway inhibitor (TFPI) in human breast and colon cancer tissue. *Thromb Haemost* 2010; 103:198-204. [\[PMID: 20062932\]](#).
  52. Belaaouaj AA, Li A, Wun TC, Welgus HG, Shapiro SD. Matrix metalloproteinases cleave tissue factor pathway inhibitor. Effects on coagulation. *J Biol Chem* 2000; 275:27123-8. [\[PMID: 10859319\]](#).

Articles are provided courtesy of Emory University and the Zhongshan Ophthalmic Center, Sun Yat-sen University, P.R. China. The print version of this article was created on 30 April 2016. This reflects all typographical corrections and errata to the article through that date. Details of any changes may be found in the online version of the article.